



## Chemical ionization using $\text{CF}_3^+$ : Efficient detection of small alkanes and fluorocarbons

Christophe Dehon<sup>a</sup>, Joël Lemaire<sup>a</sup>, Michel Heninger<sup>b</sup>, Aurélie Chaput<sup>b</sup>, Hélène Mestdagh<sup>a,\*</sup>

<sup>a</sup> Laboratoire de Chimie Physique, Université Paris-Sud/CNRS (UMR 8000), Bât. 350, Université Paris-Sud, F-91405 Orsay, France

<sup>b</sup> AlyXan, Bât. 207B, Université Paris-Sud, F-91405 Orsay, France

### ARTICLE INFO

#### Article history:

Received 30 July 2010

Received in revised form

28 September 2010

Accepted 29 September 2010

Available online 8 October 2010

#### Keywords:

Chemical ionization

Quantitative analysis

FTICR mass spectrometry

Alkanes

Fluorocarbons

### ABSTRACT

The trifluoromethyl ion  $\text{CF}_3^+$  is evaluated as a chemical ionization (CI) precursor in a compact Fourier Transform Ion Cyclotron Resonance (FTICR) mass spectrometer. It reacts with alkanes by hydride abstraction allowing characterization and quantification of alkanes up to C4 and cyclic. With larger alkanes fragmentation occurs. Fluorocarbons react by fluoride abstraction. Rate coefficients have been measured for reaction with alkanes, fluoroalkanes, chlorofluoroalkanes as well as several common VOCs. Use of  $\text{CF}_3^+$  for trace analysis in air has been tested on an air sample containing traces of acetone, toluene, benzene and cyclohexane. The results are consistent with those obtained with  $\text{H}_3\text{O}^+$  precursor and allow additional cyclohexane quantification.

© 2010 Elsevier B.V. All rights reserved.

### 1. Introduction

Real time analysis of traces of Volatile Organic Compounds (VOCs) in air is a crucial need for environmental and industrial analysis. Mass spectrometry is a versatile and sensitive tool for detection of VOCs, provided it is associated with a soft and selective ionization technique such as an ion-molecule reaction with a suitable precursor ion, referred as chemical ionization (CI) [1]. In a trace analysis context, the term “chemical ionization” means that the sample interacts with a unique, well-identified precursor ion under well-defined pressure and time conditions so that quantitative information is obtained. CI techniques using various precursors have been widely used for atmospheric trace gas measurements [2]. The most general CI reaction for VOC analysis is Proton Transfer Reaction (PTR) [3]. It has been associated with several types of mass spectrometers [4–7] and found numerous applications such as food and aroma components analysis [8], environmental analysis [9], and atmospheric research [10]. Recent areas of PTRMS study are medical sciences [11] and detection of warfare agents [12,13] or explosives [14]. Since it is a soft ionization technique resulting in little or no fragmentation, identification is made directly from the mass of the observed ions and can benefit from high mass resolution techniques leading to the molecular formula of the ions. However

PTRMS does not allow detection of compounds of very low basicity such as alkanes or haloalkanes. For this purpose, ion  $\text{O}_2^+$  may be an interesting CI reagent since it reacts with alkanes [15] and with some halocarbons [16,17] by charge transfer. However, extensive fragmentation makes its use difficult for identification.

Alkane CI characterization has been also achieved with ionic metal complexes as CI precursors, namely  $\eta^5\text{-(C}_5\text{H}_5\text{)Co}^+$  ion which reacts with alkanes by  $\text{H}_2$  loss [18], and  $\text{ClMn(H}_2\text{O)}^+$  ion reacting by  $\text{H}_2\text{O}$  ligand substitution [19], both without notable carbon-carbon bond fragmentation.

The aim of the present work is to test the potentialities of trifluoromethyl ion  $\text{CF}_3^+$  as a CI reagent for detection of alkanes and fluorocarbons present as trace compounds in air. This ion is potentially interesting since it has been reported to react with alkanes RH by hydride abstraction leading to the  $\text{R}^+$  ion [20], with  $m/z = M - 1$  for an alkane of mass  $M$ . Therefore this reaction may lead to its molecular formula. Analysis of dilute samples in air is likely possible, since no reactivity of  $\text{CF}_3^+$  with air major components has been reported. This ion is also reported to be unreactive with water [21]. According to a recent study, the ionization energy of  $\text{CF}_3$  lies in the range 9.0–9.1 eV [22], which is lower than the 12–15 eV ionization energies of  $\text{O}_2$ ,  $\text{N}_2$ , Ar,  $\text{H}_2\text{O}$  and than the ionization energies of most organic molecules (9–12 eV), confirming that  $\text{CF}_3^+$  cannot undergo charge transfer with these molecules. However,  $\text{CF}_3^+$  displays other types of reactivity with most organic molecules: small alkenes react by addition followed by HF elimination and/or react by hydride abstraction [23], aromatic hydrocarbons react by elec-

\* Corresponding author. Tel.: +33 01 69 15 56 08; fax: +33 01 69 15 61 88.  
E-mail address: [helene.mestdagh@u-psud.fr](mailto:helene.mestdagh@u-psud.fr) (H. Mestdagh).

trophilic addition followed by HF elimination [24], charge transfer being reported under more energetic conditions [25]. The reactions of  $\text{CF}_3^+$  with amines [26], phenols and various aromatics containing oxygen [27] or nitrogen [28] have been studied and often lead to several products. Carbonyl compounds react according to a characteristic “metathesis” reaction in which the  $\text{C}=\text{O}$  group is replaced by a  $\text{C}^+-\text{F}$  group, neutral  $\text{COF}_2$  being eliminated [29–33]. In most cases further fragmentations occur. Since they do not allow for easy determination of the analyte molecular formula, the reactions of  $\text{CF}_3^+$  with oxygen- or nitrogen-containing molecules seem unsuitable for analytical purposes. More interestingly for analytical purpose, the trifluoromethyl ion is also reported to react with some haloalkanes, by halide [34] or hydride [35] transfer.

In the present study, the use of  $\text{CF}_3^+$  as a CI reagent for alkane and fluoroalkane detection under CI-FTICR conditions is investigated: it includes characterization of  $\text{CF}_3^+$  reactivity under the analysis conditions, determination of the relevant rate coefficients and application to quantitative analysis of test samples diluted in air.

The experimental design used for this study is a compact Fourier Transform Ion Cyclotron Resonance (FTICR) mass spectrometer based on a structured permanent magnet. These recently developed instruments [36] have been applied successfully to PTR analysis of VOC traces in air [37,38]. They are particularly suitable for CIMS analysis, due to the following points: (i) owing to the mass resolution of FTICR technique, the molecular formula of each detected ion can be determined, improving analyte identification; (ii) since the ions are trapped in the ICR cell, they can be submitted to a sequence of operations (preparation by electron ionization, mass selection using selective ion ejection, chemical reaction, etc.) allowing clean preparation of a variety of CI reagent ions; and (iii) in the case of PTR, the CI-FTICR technique has proven reliable for quantitative analysis of complex mixtures [39].

## 2. Experimental

### 2.1. The MICRA and BTrap mass spectrometers

The MICRA mass spectrometer has been described previously [36]. Briefly, it is a compact, transportable FTICR mass spectrometer based on a structured permanent magnet weighing ca. 20 kg and yielding an homogeneous 1.25 T magnetic field. Two gas inlet lines are used to introduce gas into the mass spectrometer, one for the neutral precursor of the CI reagent ions, the other for the sample. Each line includes a three-way pulsed valve that directs the gas flow either to the mass spectrometer main vacuum chamber or to a gas inlet evacuation line: this configuration allows for sending controlled gas pulses into the ICR cell, and avoids pressure surges. Each measurement involved a programmed sequence of operations as described below. The BTrap mass spectrometer, built by LCP laboratory and AlyXan company [40], is similar to MICRA but has been optimized for trace analysis. One of its gas inlets is appropriate for gas sampling from a flow at atmospheric pressure, via two stages of pressure reduction: a leak valve and a 0.5 mm i.d. dimensioned capillary tube.

In the present work MICRA is used for kinetic studies allowing rate coefficient determination. The samples are introduced as pure gases at low pressure: the pressure range during sample admission in the cell is  $10^{-7}$ – $10^{-6}$  Torr. Test experiments of trace analysis in air are performed with BTrap: standard mixtures of compounds diluted in air with a known mixing ratio close to 50 ppm are sampled in the cell, at a pressure in the  $10^{-4}$ – $10^{-5}$  Torr range (typically  $8 \times 10^{-5}$  Torr during introduction).

### 2.2. Analytical sequence

The  $\text{CF}_3^+$  ions are produced in the cell by electron ionization of  $\text{CF}_4$  at a typical pressure of  $10^{-6}$  Torr using a 40 eV electron beam:  $\text{CF}_4 + \text{e}^- \rightarrow \text{CF}_3^+ + \text{F} + 2\text{e}^-$

The succession of precursor ion preparation, chemical ionization reaction and ion detection leading to the mass spectrum is carried out according to a programmed operating sequence. The typical sequence used for kinetic studies is scheduled as follows. The steps are listed in consecutive order, with their duration indicated in parentheses.

- 1 (20 ms)—Introduction of  $\text{CF}_4$  (a few  $10^{-6}$  Torr).
- 2 (2 ms)—Electron ionization of  $\text{CF}_4$ .
- 3 (20 ms)—Second introduction of  $\text{CF}_4$  for  $\text{CF}_3^+$  ion cooling (a few  $10^{-6}$  Torr).
- 4 (>200 ms)—Delay for complete pumping of the cell before sample introduction.
- 5 (Variable duration)—Introduction of the neutral sample ( $10^{-7}$ – $10^{-5}$  Torr): during this stage, the analytes are converted to ions by reaction with  $\text{CF}_3^+$ . The duration assigned to this stage is the reaction time. The amount of gas introduced has been shown to remain proportional to the valve opening pulse duration, including the case of short pulses for which the instantaneous pressure does not follow a square temporal profile and the static pressure limit obtained at long opening durations is far from being reached [36].
- 6 (>200 ms)—Delay for complete pumping of the cell: this delay allows the pressure to fall below  $10^{-8}$  Torr, which ensures a satisfying detection.
- 7 (50 ms)—RF excitation and detection of the signal: the ion cyclotron frequencies are excited using RF pulses, leading to large radius coherent motion of the ions. Each ion is rotating accordingly to its cyclotron frequency. The amplified image current transient signal is acquired for 50 ms. Depending on the mass resolution needed, data treatment may cover only part of the signal (10–50 ms).
- 8 (2 ms)—Ion quench: all the ions in the cell are ejected by an intense RF excitation.

The total duration of each sequence is 4 s. For each value of the reaction time, this sequence is repeated 5–50 times for transient signal averaging, improving the signal-to-noise ratio. Then the reaction time is incremented so as to record the temporal evolution of the reaction. A 10 ms increment is generally used.

### 2.3. Mass calibration

Due to its high mass accuracy, FT-ICR spectrometry makes identification of the molecular formulae possible.

Experimental masses are obtained from the observed frequencies  $\nu$  using a two-parameter calibration law  $m = A/\nu + B/\nu^2$  [41,42]. The  $A$  and  $B$  parameters are adjusted using either ions of known molecular formula present in the mixture or ions from chemical standards introduced for calibration purpose. In the present work, mass calibration was conveniently carried out using the precursor ion  $\text{CF}_3^+$  ( $m/z$  68.9952) and  $\text{H}_3\text{O}^+$  ion ( $m/z$  19.0184), terminal ion from electron ionization of the residual gas consisting of water.

For all identified compounds the difference between experimental and calculated masses was less than  $5 \times 10^{-3}$  u.

### 2.4. Pressure measurement

Knowledge of the sample pressure in the cell is crucial, since it is required for rate coefficient determination as well as for concentration measurement in air. The sample pressure in the reaction cell was measured using a Bayard–Alpert ionization gauge. The pressure

read was multiplied by a correcting factor which is the product of a constant, device-dependent term and a gas-dependent term. The former term is mainly related to the influence of the magnetic field on the gauge indications, while the latter reflects the sensitivity variation of the ionization gauge with the nature of the gas, since the gauge is normally calibrated for air. For trace analysis using Btrap the gas is air in all cases: the correcting factor is due exclusively to the magnetic field, and can be measured once for all. Since the cell is removable from the magnet bore via an axial screw system, comparison of the gauge indication  $P_B$  in the magnetic field and  $P_0$  without magnetic field was easily performed, leading to linear calibration curves  $P_0 = AP_B$  with  $A = 1.88 \pm 0.05$ . Pressure measurement for kinetic studies is less simple due to the gas-dependent term. Therefore, the global correction factor for methane was evaluated (by calibration measurements) using the reaction of  $\text{CH}_4^+$  with  $\text{CH}_4$  which has a well-known rate coefficient [43]. The gas-dependent term is proportional to the ionization cross section of the gas, which has been shown to be proportional to its molecular polarizability [44]. The gas correction factors with respect to nitrogen are reported by ionization gauge manufacturers for several gases among which methane [45]. The unreported factors were evaluated as the ratio of the polarizability of the molecule to that of nitrogen. If not available from data banks [46], the polarizabilities were evaluated using Miller empirical method [47]. This method involves a sum of components related to each atom with a given hybridization. It has been shown to lead to reliable results (2% average difference with reported experimental value) in numerous cases including halogenated molecules.

### 2.5. Kinetic data analysis and rate coefficient determination

The intensity of each ion signal is normalized to the total ion signal (sum of the ions with significant intensities) and plotted against reaction time. For the  $\text{CF}_3^+$  precursor ion the expected curve corresponds to an exponential decay with the apparent constant  $k_{\text{ap}} = k[M]$ , where  $k$  is the reaction rate coefficient and  $[M]$  the reactant gas concentration in the cell, proportional to pressure. With all reactants the relative intensity of  $\text{CF}_3^+$  actually followed an exponential decrease, providing the  $\text{CF}_3^+$  ions had been correctly cooled by collisions with  $\text{CF}_4$ .

As shown by previous studies, the amount of gas delivered in a gas pulse of programmed time length  $t$  is actually proportional to  $(t + t_0)$  rather than  $t$ . The time shift  $t_0$  depends on the gas pressure and does not exceed a few milliseconds. Therefore the abundance curve of  $\text{CF}_3^+$  is best fitted by the following equation, where  $k_{\text{ap}}$  and  $t_0$  are two adjustable parameters:

$$(\text{CF}_3^+) = \exp(-k_{\text{ap}}(t + t_0))$$

If the reaction leads to more than one product, the branching ratios  $\alpha_1, \dots, \alpha_n$  are then obtained by fitting the abundance curves of each of the  $(n - 1)$  most abundant reaction product  $\text{P}_i^+$  by equations such as the following, where  $\alpha_i$  is the adjustable parameter:

$$(\text{P}_i^+) = \alpha_i (1 - \exp(-k_{\text{ap}}(t + t_0)))$$

The value of  $\alpha_n$ , resulting from the constraint  $\sum \alpha_i = 1$ , is checked to fit the last curve.

In some cases mentioned in text, secondary reactions were observed, and taken in account in the kinetic analysis.

For several of the ion-molecule reactions the rate coefficients are compared with the capture rate coefficients, which were evaluated according to Su and Chesnavich [48]. This method requires the knowledge of the polarizability and the dipole moment of the reactant molecule.

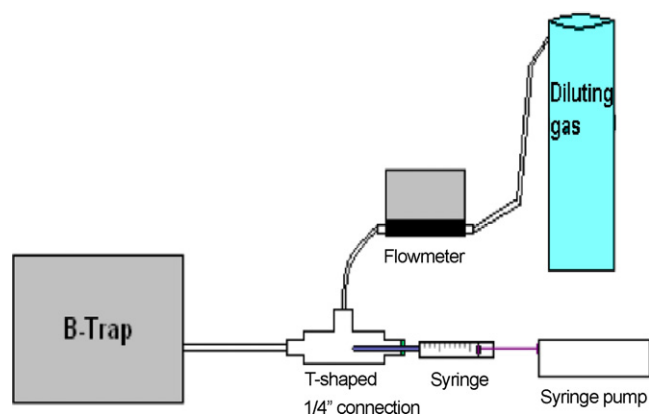


Fig. 1. Scheme of the experimental setup used for test sample preparation.

### 2.6. Trace analysis in air

For preparation of test samples in air, a system delivering known and variable amounts of VOCs in an air flow was required. The device illustrated in Fig. 1 was proved to be appropriate for this purpose. It allows for vaporizing a liquid VOC in a gas flow adjusted between 0.2 and 4 L/min by a flowmeter (usual setting 0.500 L/min), at a constant rate adjusted via a syringe pump between 23 pL/min (0.5  $\mu\text{L}$  syringe) and 26 mL/min (60  $\mu\text{L}$  syringe).

The operating sequence used in BTrap is close to the sequence used for kinetic studies in MICRA, except that the reaction time is adjusted to a fixed value. The choice of the reaction time depends on the introduction pressure and the concentrations to be detected. Its optimum value corresponds to consumption of ca. 20–30% of the precursor ion, which represents a compromise between two needs: high signal-to-noise ratio favored by a high reaction yield, and negligible secondary reactions obtained for a low reaction yield [39]. For the experiments performed in this work, the reaction time is typically 500 ms, for a sample pressure of  $2.5 \times 10^{-5}$  Torr in the cell and analyte mixing ratio in the 0–150 ppm range. Since the signal-to-noise ratio may be low for the products, the absolute intensities are corrected from noise before further data analysis, by subtracting the average noise measured in the absence of ions.

## 3. Results and discussion

### 3.1. Preparation and reaction conditions of the $\text{CF}_3^+$ ions

As reported in the literature [21], trifluoromethyl ions are easily obtained from electron ionization of  $\text{CF}_4$ . The internal energy of the  $\text{CF}_3^+$  reactant ions must be as low as possible, so that clean first-order and reproducible reaction kinetics are obtained. Cooling of the excited  $\text{CF}_3^+$  ions resulting from electron ionization is effected by a  $\text{CF}_4$  pulse allowing collisional deactivation of excited states and thermalization of the  $\text{CF}_3^+$  kinetic energy. If the  $\text{CF}_3^+$  ions are not sufficiently cooled, they do not react according to first-order kinetics.

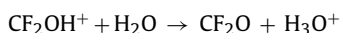
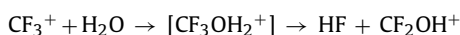
When  $\text{CF}_3^+$  ions were trapped in the presence of ambient air ( $10^{-4}$  Torr), no reaction of  $\text{CF}_3^+$  with  $\text{N}_2$ ,  $\text{O}_2$  or Ar was detectable even at long reaction time (several seconds). No reaction with  $\text{H}_2\text{O}$  was detectable either under these conditions, corresponding to a  $\text{H}_2\text{O}$  mixing ratio of ca. 1%. However, when trapping  $\text{CF}_3^+$  ions with pure water vapor at a pressure of  $10^{-4}$  Torr, slow disappearance of  $\text{CF}_3^+$  was observed, while  $\text{H}_3\text{O}^+$  ions appeared. A closer look at the spectrum showed the presence of a very minor ion with mass 67.000 u, corresponding to the molecular formula  $\text{CF}_2\text{OH}^+$ . Therefore, we conclude to slow reaction of  $\text{CF}_3^+$  with water, followed by

**Table 1**  
Reactivity of  $\text{CF}_3^+$  with simple alkanes.

Alkane	Product ion(s) ( $m/z$ )—branching ratio in %	Secondary products	Rate constant <sup>a</sup>	Capture rate constant <sup>a</sup>	Literature [20]
Methane $\text{CH}_4$	No reaction	–	–	–	n.r. [23]
Ethane $\text{C}_2\text{H}_6$	$\text{C}_2\text{H}_5^+$ (29)	–	0.32	1.08	0.37
Propane $\text{C}_3\text{H}_8$	$\text{C}_3\text{H}_7^+$ (43)	–	0.50	1.14	0.59
Butane $\text{C}_4\text{H}_{10}$	$\text{C}_4\text{H}_9^+$ (57)	–	0.62	1.21	0.75
Pentane $\text{C}_5\text{H}_{12}$	$\text{C}_3\text{H}_7^+$ (43)	$\text{C}_5\text{H}_{11}^+$ (71)	0.89	1.25	0.89
Hexane $\text{C}_6\text{H}_{14}$	$\text{C}_3\text{H}_7^+$ (43) – 45% $\text{C}_4\text{H}_9^+$ (57) – 55%	$\text{C}_6\text{H}_{13}^+$ (85)	0.86	1.30	1.05
Cyclohexane $\text{C}_6\text{H}_{12}$	$\text{C}_6\text{H}_{11}^+$ (83)	–	1.26	1.26	1.14
2,2-Dimethylbutane $\text{C}_6\text{H}_{14}$	$\text{C}_2\text{H}_5^+$ (29) – 1% $\text{C}_3\text{H}_7^+$ (43) – 34% $\text{C}_4\text{H}_9^+$ (57) – 65%	$\text{C}_6\text{H}_{13}^+$ (85)	0.98	1.30	–
Heptane $\text{C}_7\text{H}_{16}$	$\text{C}_2\text{H}_5^+$ (29) – 10% $\text{C}_4\text{H}_9^+$ (57) – 90%	–	0.93	1.36	1.18
Octane $\text{C}_8\text{H}_{18}$	$\text{C}_4\text{H}_9^+$ (57) – 44% $\text{C}_5\text{H}_{11}^+$ (71) – 52% $\text{C}_6\text{H}_{13}^+$ (85) – 4%	–	0.88	1.42	1.37
Decane $\text{C}_{10}\text{H}_{22}$	$\text{C}_4\text{H}_9^+$ (57) – 30% $\text{C}_5\text{H}_{11}^+$ (71) – 35% $\text{C}_6\text{H}_{13}^+$ (85) – 34%	–	0.81	1.50	–

<sup>a</sup> Rate constant in  $10^{-9}$  molecule $^{-1}$  cm $^3$  s $^{-1}$ .

proton transfer reaction:



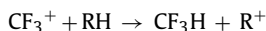
The first step has been shown to be thermodynamically favored although it was not observed [21], and to involve easy HF loss via isomerization of  $\text{CF}_3\text{OH}_2^+$  to the more stable  $(\text{HF})\text{CF}_2\text{OH}^+$  complex [49]. Since the proton affinity (PA) of  $\text{CF}_2\text{O}$  (667 kJ mol $^{-1}$ ), is lower than the PA of water (691 kJ mol $^{-1}$ ), the second step is thermodynamically favored, and likely very fast as most proton transfer reactions.

Since the relative amount of  $\text{CF}_2\text{OH}^+$  remains negligible during the reaction, the rate coefficient of  $\text{H}_3\text{O}^+$  formation can be considered as equal to the rate coefficient of the first step. It was measured by following the reaction kinetics, leading to the value  $k_{\text{H}_2\text{O}} = 1 \times 10^{-12}$  molecule $^{-1}$  cm $^3$  s $^{-1}$ .

### 3.2. Reactivity of $\text{CF}_3^+$ with alkanes

The reactivity of  $\text{CF}_3^+$  with simple alkanes has been investigated under FTICR conditions. The results are summarized in Table 1. Fig. 2 shows an example of kinetic study using small time increments.

All the alkanes tested react with  $\text{CF}_3^+$ , with the exception of methane. For C2–C4 alkanes and cyclohexane, the reaction can be written as follows:



Methane could have been expected to react by a similar H abstraction since it is exothermic by 33 kJ mol $^{-1}$  [50,51]. No  $\text{CH}_3^+$  ion was detected under the conditions used, leading to an upper limit of  $10^{-13}$  molecule $^{-1}$  cm $^3$  s $^{-1}$  for the reaction rate coefficient.

Pentane undergoes complete fragmentation to  $\text{C}_3\text{H}_7^+$ , with ethene loss:



Higher alkanes are also fragmented to C2–C6 ions. Fragmentations leading to ions with less than four carbon atoms, or to ethene loss, seem to be avoided when other possible pathways are available. Ions arising from hydride loss on the alkanes are actually detected in some cases such as hexane, but the kinetic study shows that they are products from secondary reactions, probably hydride

abstraction by the fragment ions on the alkane molecule. Therefore these informative ions, the formation of which requires two successive reactions with the alkane, are not likely to be formed under trace analysis conditions.

### 3.3. Reactivity of $\text{CF}_3^+$ with fluoroalkanes and chlorofluoroalkanes, comparison with $\text{O}_2^+$

The results concerning the reactivity of  $\text{CF}_3^+$  with some representative HFCs and CFCs are summarized in Table 2.

The reactions observed consist in halide abstraction, as exemplified by the  $\text{CF}_2\text{Cl}_2$  reactions:

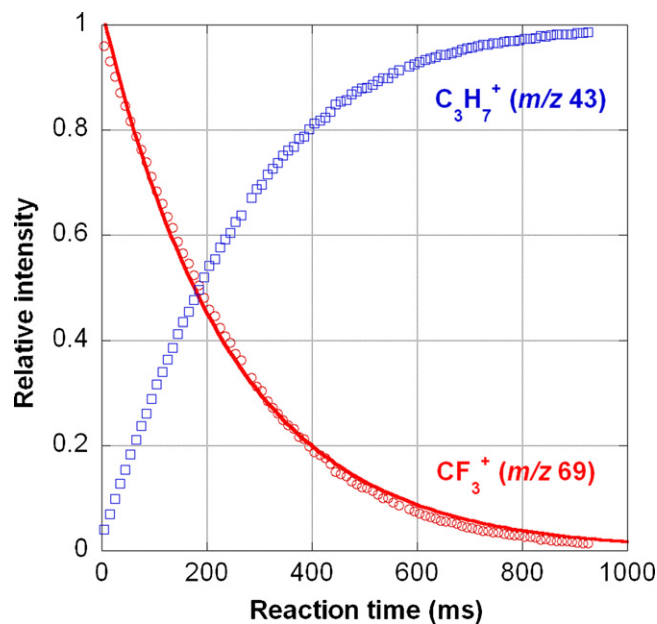
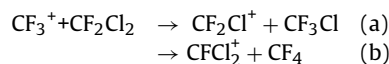


**Fig. 2.** Kinetics of the reaction of  $\text{CF}_3^+$  with propane at pressure  $3.4 \times 10^{-7}$  mbar (corrected value): dependence of ion distribution with reaction time. The solid line is an exponential fit of  $\text{CF}_3^+$  decay, corresponding to the time shift  $t_0 = -7$  ms and apparent rate constant  $k_{\text{ap}} = 4.1 \times 10^{-3}$  ms $^{-1}$ .

**Table 2**  
Reactivity of  $\text{CF}_3^+$  with fluoroalkanes.

Compound	Product ion(s) ( $m/z$ )—branching ratio in %	Reaction enthalpy ( $\text{kJ mol}^{-1}$ )	Rate constant <sup>a</sup>	Capture rate constant <sup>a</sup>
$\text{CF}_2\text{Cl}_2$ (R12)	$\text{CF}_2\text{Cl}^+$ (85, 87) 90%	−66	0.57	1.05
	$\text{CFCl}_2^+$ (101, 103, 105) 10%	−144		
$\text{CHF}_2\text{Cl}$ (R22)	$\text{CHFCl}^+$ (67, 69 <sup>b</sup> ) 50%	−110	1.32	1.46
	$\text{CHF}_2^+$ (51) 50% <sup>c</sup>	−39		
	$\text{C}_2\text{H}_3\text{F}_2^+$ (65)	−143		
$\text{CH}_3\text{—CF}_3$ (R143a)	$\text{C}_2\text{H}_2\text{F}_3^+$ (83)	−105	1.10	1.80
$\text{F}_2\text{CH—CF}_3$ (R125)	$\text{C}_2\text{HF}_4^+$ (101)	−64	1.14	1.40
$\text{ClCF}_2\text{—CF}_2\text{Cl}$ (R114)	$\text{C}_2\text{F}_4\text{Cl}^+$ (135, 137) 85%		1.10	1.06
	$\text{C}_2\text{F}_3\text{Cl}_2^+$ (151, 153, 155) 15%			

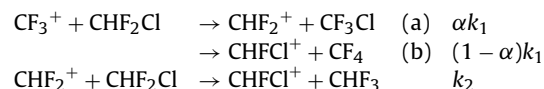
<sup>a</sup> Rate constant in  $10^{-9} \text{ molecule}^{-1} \text{ cm}^3 \text{ s}^{-1}$ .<sup>b</sup> The intensity of this ion is not measurable because its  $m/z$  is the same as this of  $\text{CF}_3^+$  reagent ion.<sup>c</sup> This ion undergoes a secondary reaction, likely fluoride abstraction from  $\text{CHF}_2\text{Cl}$  (see text and Fig. 3).

The product distributions reported in Table 2 show that chloride abstraction occurs preferentially to fluoride abstraction, itself preferential over hydride abstraction. The latter is not observed on the HFCs studied here.

The origin of this  $\text{Cl} > \text{F} > \text{H}$  reactivity order has a kinetic rather than thermodynamic origin, since most of these reactions are exothermic, with  $\text{F} > \text{H} > \text{Cl}$  in order of increasing exothermicity. The reaction enthalpies of the different channels observed, determined from Refs. [50–53] are given in Table 2. The unobserved hydride abstraction reactions on R22, R143a, R134a and R125 correspond to reaction enthalpies of −65, −15, +91, and +25  $\text{kJ mol}^{-1}$ , respectively.

In the case of R22 there is a mass overlap at  $m/z$  69 between the  $\text{CF}_3^+$  reactant ( $m/z$  68.995) and the  $\text{CH}^{37}\text{ClF}^+$  product ( $m/z$  68.972), so that the parent ion is not expected to decrease to zero. High resolution mass measurements were not attempted, since data analysis using low resolution spectra and taking this overlap into account appears as a more accurate method for kinetic studies. Besides, a secondary reaction is observed, corresponding to formation of  $\text{CHClF}^+$  from  $\text{CHF}_2^+$ . When increasing the reaction time, the relative intensity of  $\text{CHF}_2^+$  primary product attains a maximum, then decreases to zero. Meanwhile an increase is observed in the rate of formation of  $\text{CHClF}^+$ , as shown in Fig. 3.

The most likely explanation lies in the following reaction scheme:



Fitting the experimental relative abundance curves by the analytical functions corresponding to this reaction scheme leads to the following values:

$$k_1 = 1.32 \pm 0.1 \times 10^{-9} \text{ molecule}^{-1} \text{ cm}^3 \text{ s}^{-1}, \quad \alpha = 0.50 \pm 0.05, \\ k_2 = 2.06 \pm 0.2 \times 10^{-9} \text{ molecule}^{-1} \text{ cm}^3 \text{ s}^{-1}.$$

Concerning the reaction of  $\text{CF}_3^+$  with R12 the present results are in agreement with an earlier study reporting formation of  $\text{CF}_2\text{Cl}^+$  and  $\text{CFCl}_2^+$  in a 80:20 branching ratio, with a global rate coefficient

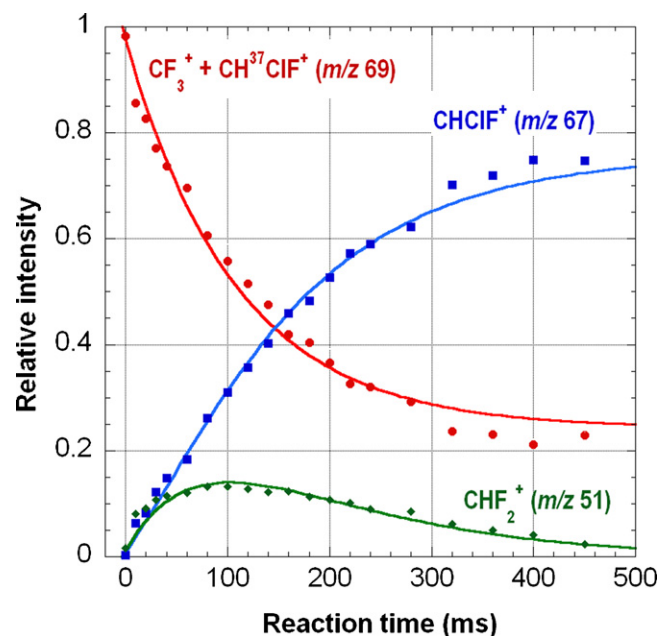


**Fig. 3.** Kinetics of the reaction of  $\text{CF}_3^+$  with  $\text{CHF}_2\text{Cl}$  (R22) at pressure  $2.5 \times 10^{-7}$  mbar (corrected value): dependence of ion distribution with reaction time. The solid lines are analytical fits of ion relative intensities according to the reaction scheme proposed in text.

of  $0.58 \times 10^{-9} \text{ molecule}^{-1} \text{ cm}^3 \text{ s}^{-1}$  [52]. Another study reports the reactivity of  $\text{CF}_3^+$  with R134a leading to  $\text{C}_2\text{H}_3\text{F}_2^+$ , and with R12 and R22 leading to chloride and fluoride abstraction products [34].

The reactivity of  $\text{O}_2^+$  with simple chlorinated hydrocarbons is known to consist in charge transfer [54] which may be followed by  $\text{Cl}$  or  $\text{HCl}$  loss [16,17]. For comparison, the reactivity of  $\text{O}_2^+$  with the above fluorinated compounds was investigated. Care was taken of ensuring correct deactivation of  $\text{O}_2^+$  electronic excited states [55]. No reaction was detected except for R12 and R114. The former yields  $\text{CF}_2\text{Cl}^+$  ( $m/z$  85, 87), the latter leads to the fol-

**Table 3**  
Reactivity of  $\text{CF}_3^+$  with common VOCs.

Compound	Product ion(s) ( $m/z$ )—branching ratio in %	Secondary products	Rate constant <sup>a</sup>	Capture rate constant <sup>a</sup>	Literature
Hexene $\text{C}_6\text{H}_{12}$	$\text{C}_3\text{H}_7^+$ (43)—65% $\text{C}_4\text{H}_7^+$ (55)—35%	$\text{C}_4\text{H}_9^+$ (57) $\text{C}_5\text{H}_{11}^+$ (71) $\text{C}_6\text{H}_{11}^+$ (83) $\text{C}_6\text{H}_{13}^+$ (85)	0.78	1.29	—
Benzene $\text{C}_6\text{H}_6$	$\text{C}_7\text{H}_5\text{F}_2^+$ (127) <sup>b</sup>	—	0.74	1.24	[24]
Toluene $\text{C}_7\text{H}_8$	$\text{C}_8\text{H}_7\text{F}_2^+$ (141) <sup>c</sup>	—	1.0	1.31	[24]
Ethanol $\text{C}_2\text{H}_6\text{O}$	$\text{C}_2\text{H}_5^+$ (29)	$\text{C}_2\text{H}_7\text{O}^+$ (47)	1.10	1.87	—
Acetone $\text{C}_3\text{H}_6\text{O}$	$\text{C}_3\text{H}_6\text{F}^+$ (61)	$\text{C}_3\text{H}_7\text{O}^+$ (59)	1.11	2.64	1.13 [56]
Propanal $\text{C}_3\text{H}_6\text{O}$	$\text{C}_3\text{H}_6\text{F}^+$ (61)—40% $\text{C}_2\text{H}_5^+$ (29)—60%	$\text{C}_3\text{H}_7\text{O}^+$ (59)	1.8	2.40	—

<sup>a</sup> Rate constant in  $10^{-9} \text{ molecule}^{-1} \text{ cm}^3 \text{ s}^{-1}$ .<sup>b</sup> Traces of  $\text{C}_6\text{H}_6^+$  ( $m/z$  78).<sup>c</sup> Traces of  $\text{C}_7\text{H}_8^+$  ( $m/z$  92).

lowing products:  $\text{CF}_2\text{Cl}^+$  ( $m/z$  85, 87) 67%,  $\text{C}_2\text{F}_4\text{Cl}_2^+$  ( $m/z$  170, 172, 174) 26%,  $\text{C}_2\text{F}_4\text{Cl}^+$  ( $m/z$  135, 137) 6%. Both rate coefficients are close to the corresponding capture rate coefficients,  $1.4 \times 10^{-9}$  and  $1.6 \times 10^{-9} \text{ molecule}^{-1} \text{ cm}^3 \text{ s}^{-1}$ , respectively. These reactions can be interpreted as initial charge transfer followed by carbon–halogen and carbon–carbon bond cleavages. The charge transfer is expected to occur when the ionization energy (IE) of the fluorocarbon is less than this of  $\text{O}_2$  (12.07 eV), which is the case only for  $\text{CF}_2\text{Cl}_2$  (IE = 12.0 eV). The unexpected reactivity of R114 (IE = 12.5 eV) was confirmed to occur even after collisional cooling of  $\text{O}_2^+$  precursor ions. Since the reported value is a vertical ionization energy [51], the adiabatic IE of R114 may be somewhat lower, which would explain its reaction with  $\text{O}_2^+$ . Consistently, the reported appearance energy of  $\text{CF}_2\text{Cl}^+$  from R114 is 12.33 eV [56].

Therefore  $\text{O}_2^+$  is of limited use as CI reagent for halocarbon analysis: while it does not react with HFCs, extensive fragmentation occurring with CFCs prevents getting quantitative information.

#### 3.4. Reactivity of $\text{CF}_3^+$ with other common VOCs: discussion of possible interferences

In order to have an idea of the behavior of  $\text{CF}_3^+$  towards a complex VOC mixture, the reactivity of  $\text{CF}_3^+$  with a few representative VOCs was investigated under the same experimental conditions. The results are summarized in Table 3.

All the VOCs tested are reactive with  $\text{CF}_3^+$ . The product ions may be identical to those formed from alkanes or fluorocarbons, which means that caution is needed when interpreting the spectrum obtained by chemical ionization of a complex mixture with  $\text{CF}_3^+$ . Examples of possible interferences are given in the following.

The  $\text{C}_2\text{H}_5^+$  ion is the only product obtained from reaction with ethanol as well as from ethane. It is likely that other small alcohols behave in the same way as ethanol, giving the product ion also obtained from the corresponding alkane. In addition,  $\text{C}_2\text{H}_5^+$  is also obtained from propanal. More generally alkyl ions of different masses are produced from a variety of neutrals such as alkanes with more than four carbon atoms, hexene and probably higher alkenes. Fluoroalkyl ions may also have an ambiguous origin, since they are produced from carbonyl compounds and can be expected to be formed from difluorinated hydrocarbons (not tested in the present study).

Therefore  $\text{CF}_3^+$  cannot be used alone for analysis of an unknown complex mixture, especially if it includes significant compounds with more than three or four carbon atoms. However, many problems of interferences between different compounds are expected to be solved by combining the use of  $\text{CF}_3^+$  with the use of  $\text{H}_3\text{O}^+$ , which allows selective detection of unsaturated and oxygen- or nitrogen-containing molecules. In particular, alcohols, alkenes and carbonyl compounds are well characterized by  $\text{H}_3\text{O}^+$  so that their contribu-

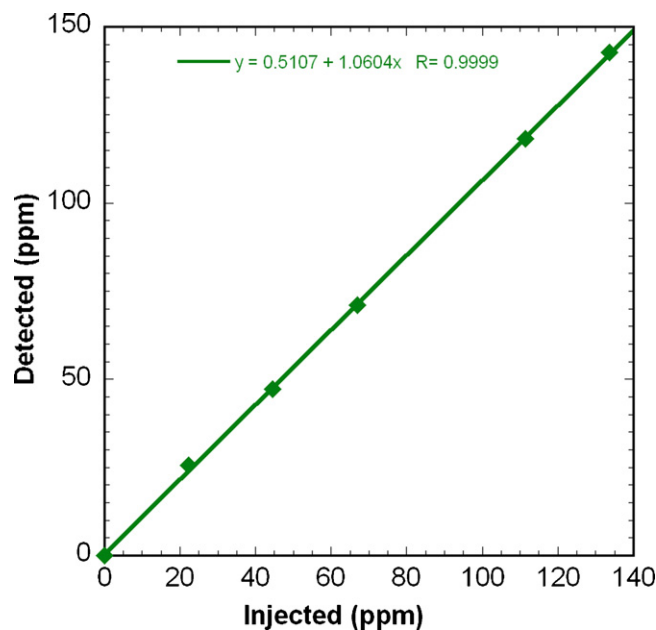


Fig. 4. Calibration curve for cyclohexane diluted in air with a variable mixing ratio.

tions can be predicted and taken into account in the  $\text{CF}_3^+$  chemical ionization spectrum.

#### 3.5. Trace analysis in air using $\text{CF}_3^+$ reagent

##### 3.5.1. Analysis of cyclohexane at variable concentration in air

In order to test the quantification ability of the method for samples diluted in air, a device delivering known and variable amounts of a given VOC in a controlled gas flow was achieved and connected to the sampling inlet line of BTrap. It is schematized in Fig. 1. This device was used to prepare mixtures containing a controlled mixing ratio of cyclohexane in air in the 10–100 ppm range, and the mixing ratio determined by CI mass spectrometry was compared to the injected mixing ratio. Fig. 4 shows the resulting calibration curve.

The calibration curve presents a good linearity. Its slope is close to unity and its intersection point with the ordinate axis close to zero. Assuming that the slope deviation from unity is due to the error on rate coefficient measurement for the reaction of  $\text{CF}_3^+$  with cyclohexane, the result indicates ca. 5% error, which is quite satisfactory for a rate coefficient measurement.

However, measuring absolute ion–molecule rate coefficients is always a delicate task, since the resulting accuracy depends on the accuracy of pressure measurement in the ICR cell, which is often poor because the ionization gauges, which are the most appropriate in the pressure range used, give a gas-dependent answer (see

**Table 4**  
Reactivity of  $\text{CF}_3^+$  with a standard VOC mixture diluted in air.

Compound	Acetone	Benzene	Toluene	Cyclohexane
Injected mixing ratio (ppm)	50	50	50	64
$\text{H}_3\text{O}^+$ analysis				
Characteristic ion ( $m/z$ )	$\text{C}_3\text{H}_7\text{O}^+$ (59)	$\text{C}_6\text{H}_7^+$ (79)	$\text{C}_7\text{H}_9^+$ (93)	–
Rate constant used <sup>a</sup>	3.90	1.95	2.27	–
Detected mixing ratio	52	56	38	–
Error percentage	+5%	+12%	–25%	–
$\text{CF}_3^+$ analysis <sup>b</sup>				
Characteristic ion ( $m/z$ )	$\text{C}_3\text{H}_6\text{F}^+$ (61)	$\text{C}_7\text{H}_5\text{F}_2^+$ (127)	$\text{C}_8\text{H}_8\text{F}_2^+$ (141)	$\text{C}_6\text{H}_{11}^+$ (83)
Detected mixing ratio	56	48	35	65
Error percentage	+12%	–4%	–30%	–1.5%

<sup>a</sup> Rate constant in  $10^{-9} \text{ molecule}^{-1} \text{ cm}^3 \text{ s}^{-1}$ , values from Refs. [39,56].

<sup>b</sup> Rate constants used are reported in Tables 1 and 3.

Section 2). Therefore, when the gas-dependent correcting factor is difficult to estimate, drawing a calibration curve from controlled mixtures of the compound in air is an interesting alternative way of determining the rate coefficient, and may be the most accurate since the pressure to be measured is basically this of air carrier gas.

### 3.5.2. Analysis of a standard gas sample in comparison with $H_3O^+$

Finally, a standard mixture of four VOCs in air was analyzed using  $CF_3^+$  and  $H_3O^+$  CI precursor ions successively. This mixture was prepared by addition of 64 ppm cyclohexane to a flow of diluting gas obtained from a commercial gas bottle containing 50 ppm each of acetone, benzene and toluene in air. The ions detected in the CI spectra and the mixing ratios derived from ion intensities are summarized in Table 4.

The expected characteristic ions are detected on each CI spectrum. Acetone, benzene and toluene can be quantified using either  $H_3O^+$  or  $CF_3^+$  precursor, with a good consistency between the mixing ratios found with both precursors. For acetone and benzene the results are close to the expected 50 ppm value. In the case of toluene both precursors indicate a mixing ratio 25–30% lower than expected. Possible reasons are toluene adsorption on surfaces of the gas bottle or of the transfer line, or toluene degradation upon storage in the gas bottle. Finally, cyclohexane is not detectable by  $H_3O^+$  but is efficiently quantified with  $CF_3^+$  at its expected mixing ratio.

## 4. Conclusions

The trifluoromethyl ion  $CF_3^+$ , very easily prepared in the FTICR cell, proves to be an interesting chemical ionization precursor for quantification of small alkanes and cyclohexane. For alkanes larger than C4 fragmentation prevents individual identification but global information on alkanes present in the mixture remains available. The  $CF_3^+$  ion is also particularly interesting as a precursor for HFCs quantification, since no other convenient CI precursor reacts with HFCs. In the present work it has been shown that  $CF_3^+$  is quite usable for trace analysis in air. However caution is needed in interpretation of CI spectra of complex mixtures, because  $CF_3^+$  reacts with practically any VOC and may lead to ions of ambiguous origin. Many of these ambiguities can be raised by associating the use of  $H_3O^+$  and  $CF_3^+$  precursors, when the sample contains mainly relatively small molecules. For detection of larger, less volatile compounds, new CI precursors will be needed. In order to improve the sensitivity, association of Membrane Introduction Mass Spectrometry (MIMS) with the use of  $CF_3^+$  precursor is currently investigated and reveals satisfying according to preliminary results.

## Acknowledgements

This work was supported by the French National Research Agency (DIRECT Project, ANR-08-SECU-003) and DGA (REI contract no. 07.34.023).

## References

- [1] A.G. Harrison, Chemical Ionization Mass Spectrometry, CRC Press, London, 1992.
- [2] L.G. Huey, Mass Spectrom. Rev. 26 (2007) 166–184.
- [3] W. Lindinger, A. Hansel, A. Jordan, Int. J. Mass Spectrom. Ion Proc. 173 (1998) 191–241.
- [4] D. Smith, P. Spanel, Mass Spectrom. Rev. 24 (2005) 661–700.
- [5] C.J. Ennis, J.C. Reynolds, B.J. Keely, L.J. Carpenter, Int. J. Mass Spectrom. 247 (2005) 72–80.
- [6] C. Warneke, J. de Gouw, E.R. Lovejoy, P.C. Murphy, W.C. Kuster, R. Fall, J. Am. Soc. Mass Spectrom. 16 (2005) 1316–1324.
- [7] L.H. Mielke, D.E. Erickson, S.A. McLuckey, M. Müller, A. Wisthaler, A. Hansel, P.B. Shepson, Anal. Chem. 80 (2008) 8171–8177.
- [8] D. Mayr, T. Mark, W. Lindinger, H. Brevard, C. Yeretdzian, Int. J. Mass Spectrom. 223–224 (2003) 743–756.
- [9] D. Smith, P. Spanel, D. Dabill, J. Cocker, B. Rajan, Rapid Commun. Mass Spectrom. 18 (2004) 2830–2838.
- [10] P. de Gouw, C. Warneke, Mass Spectrom. Rev. 26 (2007) 223–257.
- [11] G.R. Harrison, A.D.J. Critchley, C.A. Mayhew, J.M. Thompson, Br. J. Anaesth. 91 (2003) 797–799.
- [12] R.L. Cordell, K.A. Willis, K.P. Wyche, R.S. Blake, A.M. Ellis, P.S. Monks, Anal. Chem. 79 (2007) 8359–8366.
- [13] F. Petersson, P. Sulzer, C.A. Mayhew, P. Watts, A. Jordan, L. Märk, T.D. Märk, Rapid Commun. Mass Spectrom. 23 (2009) 3875–3880.
- [14] C.A. Mayhew, P. Sulzer, F. Petersson, S. Haidacher, A. Jordan, L. Märk, P. Watts, T.D. Märk, Int. J. Mass Spectrom. 289 (2010) 58–63.
- [15] P. Spanel, D. Smith, Int. J. Mass Spectrom. Ion Proc. 181 (1998) 1–10.
- [16] P. Spanel, D. Smith, Int. J. Mass Spectrom. 184 (1999) 157–181.
- [17] P. Spanel, D. Smith, Int. J. Mass Spectrom. 189 (1999) 213–223.
- [18] J.L. Campbell, M.N. Fiddler, K.E. Crawford, P.P. Cqamana, H.I. Kenttamaa, Anal. Chem. 77 (2005) 4020–4026.
- [19] P. Duan, K. Ojan, S.C. Habicht, D.S. Pinkston, M. Fu, H.I. Kenttamaa, Anal. Chem. 80 (2008) 1847–1853.
- [20] S.G. Lias, J.R. Eyler, P. Ausloos, Int. J. Mass Spectrom. Ion Phys. 19 (1976) 219–239.
- [21] F. Grandinetti, G. Occhiucci, M.E. Crestoni, S. Fornarini, M. Speranza, Int. J. Mass Spectrom. Ion Proc. 127 (1993) 123–135.
- [22] E.E. Ferguson, T.M. Miller, A.A. Viggiano, J. Chem. Phys. 118 (2003) 2130–2134.
- [23] R.A. Morris, E.R. Brown, A.A. Viggiano, J.M. Van Doren, J.F. Paulson, V. Motevalli, Int. J. Mass Spectrom. Ion Proc. 121 (1992) 95–109.
- [24] M. Tsuji, M. Aizawa, Y. Nishimura, Bull. Chem. Soc. Jpn. 68 (1995) 3497–3505.
- [25] A.E.P.M. Sorrihla, L.S. Santos, F.C. Gozzo, R. Sparrapan, R. Augusti, M.N. Eberlin, J. Phys. Chem. A 108 (2004) 7009–7020.
- [26] F. Grandinetti, G. Occhiucci, M.E. Crestoni, S. Fornarini, M. Speranza, Int. J. Mass Spectrom. Ion Proc. 127 (1993) 137–146.
- [27] M. Tsuji, R. Aizawa, Y. Nishimura, Bull. Chem. Soc. Jpn. 69 (1996) 147–156.
- [28] M. Tsuji, M. Aizawa, H. Ujita, Y. Nishimura, Bull. Chem. Soc. Jpn. 68 (1995) 2385–2392.
- [29] P. Ausloos, S.G. Lias, J.R. Eyler, Int. J. Mass Spectrom. Ion Phys. 18 (1975) 261–271.
- [30] D. Leblanc, J. Kong, P.S. Mayer, T.H. Morton, Int. J. Mass Spectrom. 219 (2002) 525–535.
- [31] P.S. Mayer, D. Leblanc, T.H. Morton, J. Am. Chem. Soc. 124 (2002) 14185–14194.
- [32] D. Leblanc, J. Kong, P.S. Mayer, T.H. Morton, Int. J. Mass Spectrom. 222 (2003) 451–463.
- [33] M. Tsuji, M. Aizawa, Y. Nishimura, Bull. Chem. Soc. Jpn. 69 (1996) 1055–1063.
- [34] J.H.J. Dawson, W.G. Henderson, R.M. O'Malley, K.R. Jennings, Int. J. Mass Spectrom. Ion Phys. 11 (1973) 61–71.
- [35] V.A. Mikhailov, M.A. Parkes, R.P. Tuckett, C.A. Mayhew, J. Phys. Chem. A 110 (2006) 5760–5771.
- [36] G. Mauclaire, J. Lemaire, P. Boissel, G. Bellec, M. Heninger, Eur. J. Mass Spectrom. 10 (2004) 155–162.
- [37] S. Sarrabi, X. Colin, A. Tcharkhtchi, M. Heninger, J. Leprovost, H. Mestdagh, Anal. Chem. 81 (2009) 6013–6020.
- [38] A.S. Tsuji, N. Blin-Simiand, M. Heninger, H. Mestdagh, P. Boissel, F. Jorand, J. Lemaire, J. Leprovost, S. Pasquiers, G. Popa, C. Postel, J. Phys. Chem. A 114 (2010) 397–407.
- [39] C. Dehon, E. Gauzere, J. Vaussier, M. Heninger, A. Tchaplaj, J. Bleton, H. Mestdagh, Int. J. Mass Spectrom. 272 (2008) 29–37.
- [40] AlyXan, [www.alyxan.com](http://www.alyxan.com).
- [41] E.B. Ledford, D.L. Rempel, M.L. Gross, Anal. Chem. 56 (1984) 2744–2748.
- [42] L.-K. Zhang, D. Rempel, B.N. Pramanik, M.L. Gross, Mass Spectrom. Rev. 24 (2005) 286–309.
- [43] V.G. Anicich, J. Phys. Chem. Ref. Data 22 (1993) 1469–1569.
- [44] R.L. Summers, NASA Technical Note NASA TN D-5285, 1969.
- [45] Varian, Multi-Gauge Controller Instruction Manual, 2001.
- [46] Handbook of Chemistry and Physics, CRC Press, 1992–1993.
- [47] K.J. Miller, J. Am. Chem. Soc. 112 (1990) 8533–8542.
- [48] T. Su, W.J. Chesnavich, J. Chem. Phys. 76 (1982) 5183.
- [49] L.J. Chyall, R.R. Squires, J. Phys. Chem. 100 (1996) 16435–16440.
- [50] H.Y. Afeefy, J.F. Liebman, S.E. Stein, Neutral thermochemical data, in: NIST Chemistry WebBook, NIST Standard Reference Database Number 69, National Institute of Standards and Technology, Gaithersburg, MD 20899, 2003, <http://webbook.nist.gov>.
- [51] S.G. Lias, J.F. Liebman, Ion energetics data, in: NIST Chemistry WebBook, NIST Standard Reference Database Number 69, National Institute of Standards and Technology, Gaithersburg, MD 20899, 2003, <http://webbook.nist.gov>.
- [52] S.G. Lias, P. Ausloos, Int. J. Mass Spectrom. Ion Phys. 23 (1977) 273–292.
- [53] D.P. Ridge, J. Am. Chem. Soc. 97 (1975) 5670–5674.
- [54] G.J. Francis, V.S. Langford, D.B. Milligan, M.J. McEwan, Anal. Chem. 81 (2009) 1595–1599.
- [55] R. Marx, S. Fenistein, G. Mauclaire, J. Lemaire, M. Heninger, Int. J. Mass Spectrom. Ion Proc. 132 (1994) 143–148.
- [56] L.M. Leyland, J.R. Majer, J.C. Robb, Trans. Faraday Soc. 66 (1970) 898–900.